



Enantioseparations on amylose tris(5-chloro-2-methylphenylcarbamate) in nano-liquid chromatography and capillary electrochromatography

Salvatore Fanali^a, Giovanni D'Orazio^a, Ketevan Lomsadze^b,
Shorena Samakashvili^b, Bezhan Chankvetadze^{b,*}

^a Institute of Chemical Methodologies, Consiglio Nazionale delle Ricerche, Area della Ricerca di Roma I, Via Salaria Km 29, 300-00015 Monterotondo Scalo (Roma), Italy

^b Department of Physical and Analytical Chemistry and Molecular Recognition and Separation Science Laboratory, School of Exact and Natural Sciences, Tbilisi State University, 0179 Tbilisi, Republic of Georgia

ARTICLE INFO

Article history:

Available online 12 September 2009

Keywords:

Enantiomers
Capillary electrochromatography
Nano-liquid chromatography
Polysaccharide-based chiral stationary phases

ABSTRACT

Amylose tris(5-chloro-2-methylphenylcarbamate) was coated onto native and aminopropylsilanized silica in order to prepare chiral stationary phases (CSP) for enantioseparations using nano-liquid chromatography (nano-LC) and capillary electrochromatography (CEC). The effect of the nature of silica, the particle size and pore diameter, the chiral selector loading onto silica, the mobile phase composition and pH, as well as separation variables such as a linear flow rate of the mobile phase, applied voltage in CEC, etc. on the separation of enantiomers was studied. It was found that CSPs based on amylose tris(5-chloro-2-methylphenylcarbamate) can be used for preparation of stable capillary columns for enantioseparations by nano-LC and CEC in combination with polar organic and aqueous–organic mobile phases. Higher peak efficiency was observed in CEC than in nano-LC.

© 2009 Elsevier B.V. All rights reserved.

1. Introduction

Capillary electrochromatography (CEC) and nano-liquid chromatography (nano-LC) have been considered as very promising techniques for analytical scale enantioseparations several years ago [1–4]. However, some stagnation of the research activity is observed in both of the above mentioned techniques in recent years, while microcolumn liquid chromatography with column internal diameters between 300 and 1000 μm is considered as an attractive technology from the viewpoint of material and cost saving and providing the opportunity for fast parallel analyses [5–8].

The most likely reasons for the decreasing research activities and applications of CEC and nano-LC for enantioseparations seem to be the following: (1) capillary columns containing effective and widely applicable chiral stationary phases (CSPs) for enantioseparations are not commercially available and their in-house preparation requires some experience and know-how; (2) particle-packed capillary columns prepared for CEC based on fused-silica contain a fragile part and may be easily destroyed; (3) sufficient research results have not been published in the last few years clearly illustrating the advantages of CEC over other chromatographic techniques. Many of the papers published on this topic

report either similar (or even lower) peak efficiency in CEC compared to chromatographic techniques. Since a CEC experiment is more demanding compared to a chromatographic one, there is no reason to perform CEC unless a clear advantage from the viewpoint of peak efficiency can be demonstrated and applied to a given practical problem. In addition, good column to column reproducibility of retention and selectivities need to be demonstrated under CEC conditions in order to increase the interest for this technique by the regulation dominated pharmaceutical industry.

In the light of the above mentioned studies for preparation of highly effective and widely applicable capillary columns for nano-LC and CEC separations of enantiomers are urgently required. In addition, the mechanism of flow generation, analyte transport and separation in CEC need to be better understood.

A large number of CSPs including brush type [9], proteins [10,11] cyclodextrins [12,13], chiral synthetic polymers [14,15], polysaccharide derivatives [16–21], etc. have been successfully used in HPLC. Among them, polysaccharide phenylcarbamate derivatives are most widely employed CSPs for enantioseparations [16–21].

The applicability of cellulose tris(3,5-dimethylphenylcarbamate) (CDMPC) for enantioseparations in open tubular capillary chromatography and CEC was demonstrated by Francotte and Jung in 1996 [22]. Open-tubular wall-coated capillary columns for nano-LC and CEC applications suffer from low sample loading capacity, low enantiomer resolving capability and low stability.

Later, silica particles modified with CDMPC [23–25], cellulose tris(3,5-dichlorophenylcarbamate) [26–28], and amylose tris(3,5-

* Corresponding author.

E-mail address: bezhan.chankvetadze@yahoo.com (B. Chankvetadze).

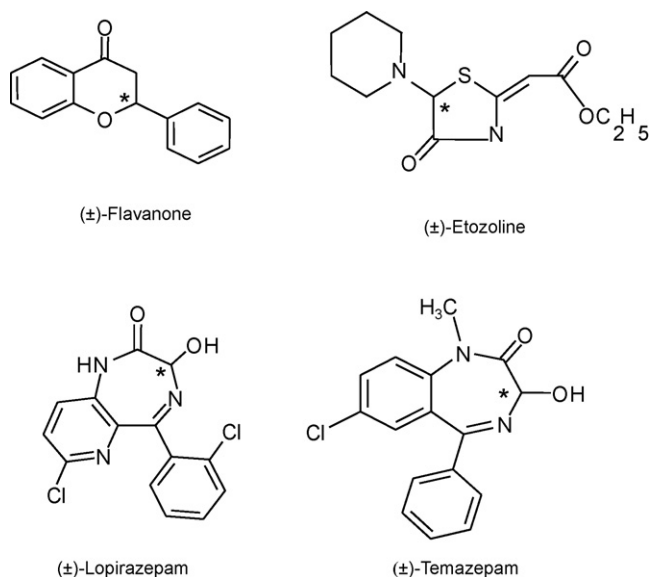


Fig. 1. Structures of chiral analytes.

dimethylphenylcarbamate) [29] were used for enantioseparations in nano-LC and CEC. The presence of modified phenylcarbamates in the polysaccharide structure may produce CSPs with different enantioselectivity depending on the type and position of the substituents on the phenyl group [15–18]. A series of phenylcarbamate derivatives having both, electron-donating and electron-withdrawing groups on the phenyl moiety exhibit interesting enantiomer resolving abilities [17,19–21,30,31]. The application of one of these new CSPs, namely cellulose tris(3-chloro-4-methylphenylcarbamate) for enantioseparations by CEC and nano-LC has been recently reported [32].

The goal of the present study was to apply another member of this new family of CSPs, namely amylose tris(5-chloro-2-methylphenylcarbamate) to the separation of enantiomers in the nano-LC and CEC modes. The effect of the surface chemistry, particle size and pore diameter of silica, its loading with the chiral selector (polysaccharide derivative), pH and composition of the mobile phase and other variables on the generation of the electroosmotic flow (EOF) and separation of enantiomers was also studied. Systematic comparisons were performed between CEC and nano-LC separations.

2. Experimental

2.1. Chemicals and samples

All chemicals were of analytical reagent grade and used as received. Methanol (MeOH), acetonitrile (MeCN), formic, acetic and hydrochloric acids and tris(hydroxymethyl)aminomethane (Tris) were purchased from Carlo Erba (Milan, Italy). Ammonium hydroxide solution (30%) was from Riedel-de Haen (Seelze, Germany). Racemic flavanone and temazepam were obtained from Sigma (St. Louis, MO, USA), while lopirazepam and etozoline were kindly provided by the Institute of Pharmaceutical and Medicinal Chemistry, University of Münster, Germany. The chemical structures of the studied racemic compounds are shown in Fig. 1. Deionized water was obtained by using the Milli-Q system (Millipore, Milford, MA, USA). Buffer solutions were prepared every week and stored at +4 °C. Mobile phases were prepared daily by mixing the suitable volumes of organic solvents, water and buffer solutions.

Stock standard solutions of the analytes of 1 mg/mL were prepared by dissolving the appropriate amount of each compounds in methanol (in the case of etozoline in acetonitrile). Working solutions were prepared by diluting the stock solutions with methanol: etozoline and temazepam to 0.1 mg/mL, flavanone to 0.05 mg/mL and lopirazepam to 0.02 mg/mL. When not in use all solutions were stored at +4 °C.

2.2. Instrumentation

An ultrasonic bath model FS 100b Decon (Hove, UK) was employed to sonicate solutions and capillary columns during the packing step. A MicroPH 2001 Meter (Crison, Barcellona, Spain) was used for pH measurements. Fused-silica capillaries (100 μm I.D. × 375 μm O.D.) were purchased from Composite Metal Services (Hallow, Worcestershire, UK). A HPLC pump (PerkinElmer Series 10, Palo Alto, CA, USA) was used for packing capillary columns.

2.2.1. CEC

In CEC experiments, an Agilent Technologies (Waldbronn, Germany) capillary electrophoresis instrument ^{3D}CE equipped with a UV–vis diode array detector (DAD) was used. Detection was performed at 214 nm. Capillary temperature was controlled by an air thermostating system. For collecting and reprocessing data the ^{3D}CE Chemstation software (Rev. A.09.01, Agilent Technologies) was used.

2.2.2. Nano-LC

Nano-LC experiments were carried out by using a laboratory assembled instrumentation consisting of an HPLC Accella[®] pump from Thermo-Finnigan (San Jose, CA, USA), a modified injector valve from Sepaserve GmbH (Münster, Germany) and on-column spectrophotometric detectors Spectra 100 and Spectra System UV 1000 from Thermo Separation Products (St. Jose, CA, USA). The valve was equipped with a 50 μL loop containing the mobile phase. Sample injection was performed by filling the sample injection loop with sample solutions and applying a pressure 10 bar for 0.2 min (the injected amount was approximately 60 nL), afterwards the injector was flushed with the mobile phase (250 μL) and filled with the mobile phase. The flow rate of mobile phase was reduced from the mL/min to the nL/min range by using a passive split system: a stainless steel T piece (Vici Valco, Houston, TX, USA) and PEEK fittings (50 cm × 130 μm I.D. from the pump and 70 cm × 50 μm I.D. for the waste position). The split was connected to the injector by a stainless steel tube (5 cm × 500 μm I.D.).

The capillary column was directly inserted into the modified injector in such a way that it was immersed practically dead volume free either in the sample solution (during sample injection) or the mobile phase (during analysis).

The data from the detector were acquired with a Shimadzu CR5A Chromatopac integrator (Kyoto, Japan) and ChromQuest version 3.0 software (Thermo Finnigan, St. Jose, CA, USA). The micro HPLC pump was operated in the isocratic mode, delivering acetonitrile at flow rate in range of 20–400 μL/min. The effective/actual in-column flow rate was experimentally estimated by using a 10 μL syringe connected to the outlet of the capillary column by a Teflon tube (TF-350; LC Packing, CA, USA) for 5 min. The measured splitting ratio was about 300. Continuous room conditioning set at 25 °C controlled the temperature of the chromatographic system.

2.3. Preparation of stationary phases

The chemical structure of the chiral selector used in these experiments is shown in Fig. 2. Amylose tris(5-chloro-2-methylphenylcarbamate) was synthesized as described previously

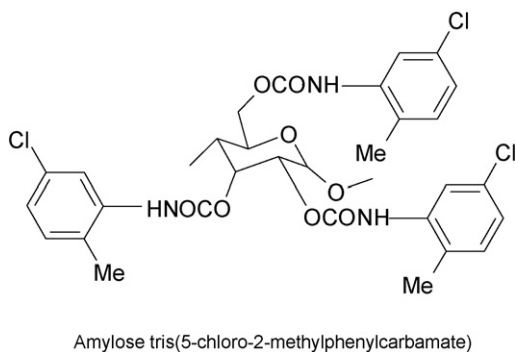


Fig. 2. Structure of amylose tris(5-chloro-2-methylphenylcarbamate).

[30]. The polysaccharide derivative was dissolved in tetrahydrofuran and coated onto silica particles of various surface chemistry, particle size and pore diameters in order to prepare CSPs used for packing the capillary columns applied in this study. The following CSPs were prepared: (i) native silica particles with nominal particle size of 5 μm and nominal pore size of 100 nm coated with 5, 10, 15 or 25% (w/w) polysaccharide derivative and (ii) aminopropylsilanized silica with 3, 5, 7, 10 μm nominal particle size and nominal pore size of 100 nm coated with the chiral selector at a concentration of 25% (w/w), as well as (iii) native silica particles with 5 μm nominal particle size and of 10, 30, 100 and 200 nm nominal pore diameter coated with the chiral selector at a concentration of 25% (w/w).

2.4. Preparation of capillary columns

The stationary phases were packed by means of the slurry packing method as described in a previous publication [32]. One end of a silica capillary (100 μm I.D. \times 375 μm O.D. \times 60 cm) was connected to a HPLC stainless steel frit (Valco, Houston, TX, USA) to retain the packing material. The other end was joined to a HPLC pre-column (50 mm \times 4.1 mm I.D., Valco, Houston, TX, USA) as reservoir of stationary phase suspension. The slurries were prepared at concentration of 50 mg/mL in methanol/water 80:20 (v/v), sonicated for 10 min and then transferred into the reservoir.

The reservoir was attached to a HPLC pump (PerkinElmer Series 10 LC, Palo Alto, CA, USA) where methanol was delivered at a flow rate of 0.9 mL/min (40 MPa, 400 bar). During the packing procedure the capillary was inserted into the ultrasonic bath. After packing about 30 cm of the capillary, the slurry was removed and the stationary phase was flushed with 5 mM NaCl in MeOH/water (80:20, v/v) for 30 min at 40 MPa. Under these conditions inlet and outlet frits were fabricated from packing material using home-made electrical hot wire filament heated at 700 $^{\circ}\text{C}$ for 5–6 s.

After this the temporary frit was removed, and the excess of stationary phase was eliminated in the back-flushing mode. A detection window was prepared close to the outlet frit by removing the polyimide coating on the capillary tube with a razor. The capillary column (25.0 and 34.0 cm packed and total length, respectively) was first flushed with a 80:20 MeOH/H₂O (v/v) mixture for 1 h to remove NaCl and then equilibrated with the mobile phase for 1 h. Before CEC runs the column was further conditioned applying a rump voltage for 1 h until observing a good baseline and a stable current. Following its use, the column was stored in the CEC instrument with the end of the capillary submerged in 80:20 MeOH/H₂O (v/v). Each capillary column was first used for CEC experiments and then for nano-LC measurements.

2.5. Calculation of chromatographic parameters

The efficiency values were measured as number of theoretical plates per meter (N/m), given by:

$$N = 5.54 \left(\frac{t_R}{w_{1/2}} \right)^{1/2} \quad (1)$$

where t_R and $w_{1/2}$ are the retention time and the peak width at half height, respectively.

The enantioresolution factors, R_s , were calculated according to the following formula:

$$R_s = 2 \frac{t_{R2} - t_{R1}}{w_1 + w_2} \quad (2)$$

where t_{R1} and t_{R2} are the retention times of the enantiomers and w was the peak width at baseline. The van Deemter equation used for calculation of A, B and C-terms was:

$$H = A + \frac{B}{u} + Cu \quad (3)$$

where H is the height equivalent to the theoretical plate HETP in μm and u is the linear velocity in $\mu\text{m}/\text{ms}$. The van Deemter's plot and A, B, C were obtained by using Curve expert 1.38 from Microsoft Corporation (<http://userpages.xfoneusa.net/~dhyams/cftp.htm>).

3. Results and discussion

3.1. Electroosmotic flow (EOF)

Since new materials were synthesized for the application in both, nano-LC and CEC, the effect of the nature and the composition of the stationary phase on the generation of the EOF was carefully studied. In addition, the mobile phase composition and pH were optimized in order to generate the most suitable EOF for achieving high efficiency and the shortest possible separation time in the CEC mode. In the capillaries packed with the material with 10 nm nominal pores size the EOF was too weak and instable most likely due to double-layer overlap within intra-particle channels [36,37]. With increasing nominal pore size of the silica from 30 to 100 nm the EOF increased as expected. However, it levelled off at 100 nm and did not increase further with increasing the nominal pore diameter to 200 nm (Fig. 3a). With increasing pore size of silica the double electric layer overlap within the intra-particle channels decreases and the EOF increases subsequently. However, at the same time the average relative surface area of the silica also decreases with increasing mean pore diameters and this may lead to the decrease of the EOF. The overall observed effect represents the sum of these two counteracting contributions. Most likely these two effects balance each other when the pore diameter of silica increases from 100 to 200 nm.

In the case of polysaccharide based CSPs up to 25% (w/w) neutral polysaccharide derivative is loaded onto the surface of silica. This may cause a significant shielding of charged groups on the surface of native and aminopropyl silanized silicas [26,27,29,33,34]. In addition, the size of the pore entrance might be eventually affected by coating the silica surface with polysaccharide derivatives. Both effects may cause a decrease of the EOF and somehow diminish the role of intra-particle flow (path) in the migration of the analyte through the packed bed. As it is shown in Fig. 3b, the EOF decreases with increasing loading of polysaccharide derivative onto the surface of silica. However, as previous electron-microscopic studies and calculations showed [26,33] the size of pore entrances are not affected significantly by coating of silica with polysaccharide phenylcarbamates.

As can be seen from Fig. 3c the increase of the background electrolyte pH caused an increase of the cathodic EOF mobility up to pH

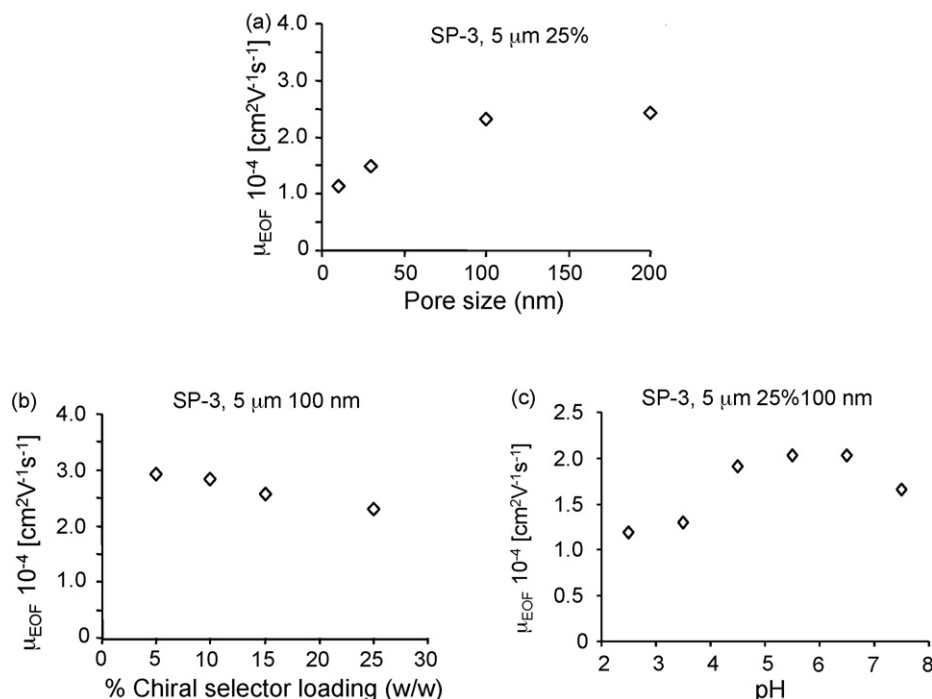


Fig. 3. Effect of (a) silica pore size, (b) chiral selector content and (c) pH of the background electrolyte on the electroosmotic flow. Experimental conditions were as follows: capillary column: 100 μm I.D. × 375 μm O.D.; L_{packed} 25.0 cm; L_{eff} 25.5 cm; stationary phase: native silica (5 μm) with different pore size and loading with amylose tris (2-chloro-5-methylphenylcarbamate). Mobile phase: (a) and (b) 500 mM NH_4Ac , pH 5.5/ $\text{H}_2\text{O}/\text{MeOH}/\text{ACN}$, 1:4:25:70 (v/v/v); (c) 500 mM buffer solution with different apparent pH/ MeOH/ACN , 1:49:50 (v/v/v); ammonium formate (pH 2.5–3.5), ammonium acetate (pH 4.5–6.5), Tris-Cl (pH 7.5); injection: 10 bar × 0.2 min and plug, 10 bar × 0.2 min, applied voltage, +15 kV; temperature: 25 °C; pressure: 10 bar on both vials.

5.5 when the capillary was packed with native silica-based CSP. The decrease of the EOF by a further increase of the buffer pH most likely relates to the different types of background electrolytes used (TRIS-buffer was used in this pH-range in order to maintain a buffering capacity) as well as to the difference in the ionic strength of applied buffers. No such decrease was observed in our previous studies with native silica-based CSPs (but with aminopropyl silica-

based CSPs) when a uniform electrolyte was used over the entire pH range studied [32,34,35]. Considering the data reported above, for further experiments with native silica-based CSPs a mobile phase with a buffer adjusted at pH 5.5 was selected.

Capillaries packed with native and aminopropyl silica coated with 25% (w/w) chiral selector were also tested in order to study the effect of the applied voltage on the generation of the EOF. By

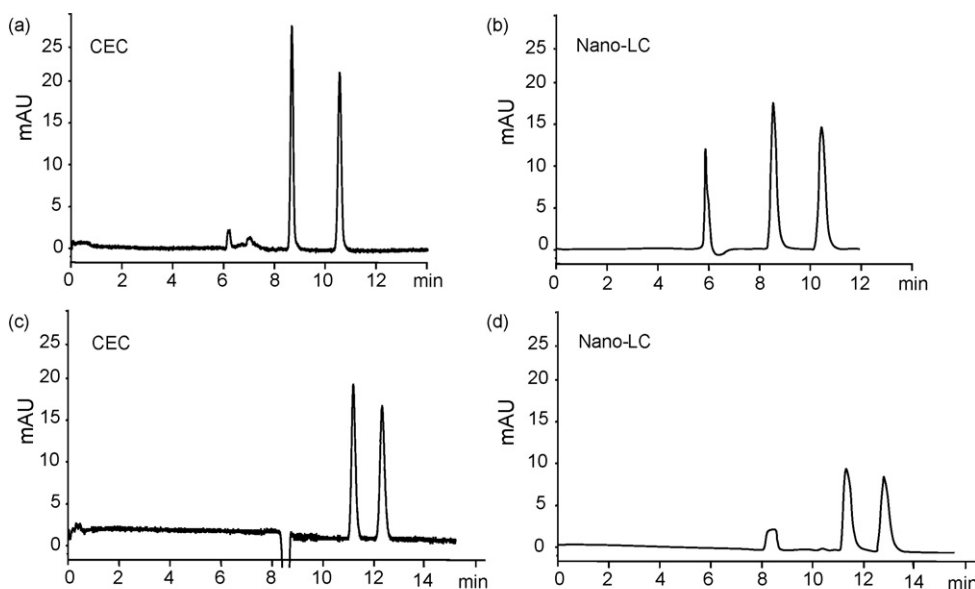


Fig. 4. Comparative enantioseparation of flavanone on native (a and b) and aminopropyl silica (c and d) (5 μm, 100 nm) coated with 25% (w/w) chiral selector by using CEC and nano-LC. Capillary column: 100 μm I.D. × 375 μm O.D.; L_{packed} 25.0 cm; L_{eff} 25.5 cm; mobile phase: (a) and (b) 500 mM NH_4Ac , pH 5.5/ $\text{H}_2\text{O}/\text{MeOH}/\text{ACN}$, 1:4:25:70 (v/v/v); (c) and (d) 500 mM NH_4Ac , pH 5.5/ MeOH/ACN , 1:49:50 (v/v/v). Nano-LC conditions: injection volume, about 60 nL; flow rate (b) 210 nL/min, (d) 170 nL/min. CEC conditions: applied voltage (a) +10 kV and (c) –15 kV. For other CEC conditions, see Fig. 3.

increasing the voltage from 10 to 25 kV (absolute value) a linear increase of the EOF mobility was observed as expected. Although a relatively high current was recorded (10 and $-7.9 \mu\text{A}$ at 25 and -25 kV , respectively), good correlation factors $r^2 = 0.9956$ and 0.9917 were observed for native and aminopropyl silica, respectively. Therefore, the negative effect of joule heating on peak dispersion can be neglected.

3.2. Comparison of native and aminopropylsilanized silica as support for chiral selector

Significant differences can be observed between polysaccharide-based CSPs prepared by coating onto native and aminopropylsilanized silica in the chromatographic separation of charged analytes. In CEC experiments this difference becomes even more significant due to the opposite direction and different strengths of the EOF generated in these capillaries.

The CEC separation of the enantiomers of flavanone with the capillary columns packed with native and aminopropylsilanized silica particles coated with 25% (w/w) chiral polymer is shown in Fig. 4. In order to observe comparable analysis times different voltages were applied while the other experimental conditions were been kept similar. The EOF observed in the capillary columns packed with native silica-based CSP was approximately 30–35% higher compared to capillary packed with CSP based on aminopropylsilanized silica. This result differs from the result observed in our previous study [34] and may be caused due to different silica materials applied in the present and previous study as well as due to the different background electrolytes used. The separation factor, as well as the plate numbers were somewhat higher in the capillary columns packed with native silica-based CSP. Some difference in the morphology of silica particles used for preparation of these two CSPs as well as in the actual loading with the chiral selector (the differences between the nominal and actual characteristics) can be responsible, in part, for these observations. It is also worth to be considered that in the capillaries packed with the CSP based on aminopropylsilanized silica a rather weak cathodic EOF generated on the fused-silica capillary wall and in the empty segment of the capillary opposes the anodic EOF generated on the surface and intra-particle channels of particles. This may cause some flow inhomogeneities and adversely affect the peak efficiency in the latter capillaries.

The relationship between these two capillary columns in nano-LC was very similar to that observed in CEC (Fig. 4). The capillary columns packed with native silica-based CSP was again advantageous over the capillary columns packed with CSP based on aminopropyl silica. This result indicates that the above mentioned effects specific for electrokinetic migration mechanism may not necessarily play the major role in the differences observed between these two CSPs. The plate numbers were approximately 3 times higher in CEC separations compared to nano-LC with both kinds of materials used (Fig. 4). This is a significant advantage of CEC over nano-LC.

3.3. The effect of particle size of silica on separation performance in nano-LC and CEC

As well documented in chromatographic as well as in CEC experiments [34,37], the peak efficiency increased with decreasing particle size in this work also for all 4 studied analytes. Since one of the major goals of this study was to follow mechanisms of increased peak efficiency in CEC compared with nano-LC, the van Deemter dependences were constructed (Fig. 5) and van Deemter coefficients calculated for both enantiomers of flavanone (Table 1). Lower A-terms were observed in CEC separations in the capillary columns packed with the material having $3 \mu\text{m}$ nominal particle size com-

Table 1
The values of van Deemter coefficients for the enantiomers of flavanone by using capillary column packed with native and aminopropyl silica of 3 and $5 \mu\text{m}$ nominal particle size. 100 nm nominal pore diameter and coated with 25% (w/w) chiral selector.

Particle size, μm	First enantiomer				Second enantiomer													
	A, μm		B, $\mu\text{m}^2/\text{ms}$		C, ms		C, ms											
	CEC Nat.	CEC APS	nano-LC, APS	nano-LC, APS	CEC Nat.	CEC APS	nano-LC, APS	nano-LC, APS										
3	1.70	2.30	13.92	2.38	1.94	5.41	1.76	3.72	14.38	1.83	1.91	22.49	2.40	2.03	4.63	2.27	4.14	16.39
5	3.78	3.32	26.95	1.52	2.18	8.10	2.72	5.95	25.99	4.92	2.33	30.04	1.34	2.23	7.46	3.25	7.19	27.99

Experimental conditions: mobile phase, native (Nat.), $500 \text{ mM NH}_4\text{Ac}$, $\text{pH } 5.5/\text{H}_2\text{O}/\text{MeOH}/\text{ACN}$, $1:4:25:70$ (v/v/v); aminopropyl (APS), $500 \text{ mM NH}_4\text{Ac}$, $\text{pH } 5.5/\text{MeOH}/\text{ACN}$, $1:49:50$ (v/v/v). CEC conditions: applied voltage, native (Nat.) $3-30 \text{ kV}$ and aminopropyl (APS) -5 to 25 kV . Nano-LC conditions: injection volume, about 60 nL ; flow rate, $100-1300 \text{ nL}/\text{min}$. For other CEC conditions, see Fig. 3a.

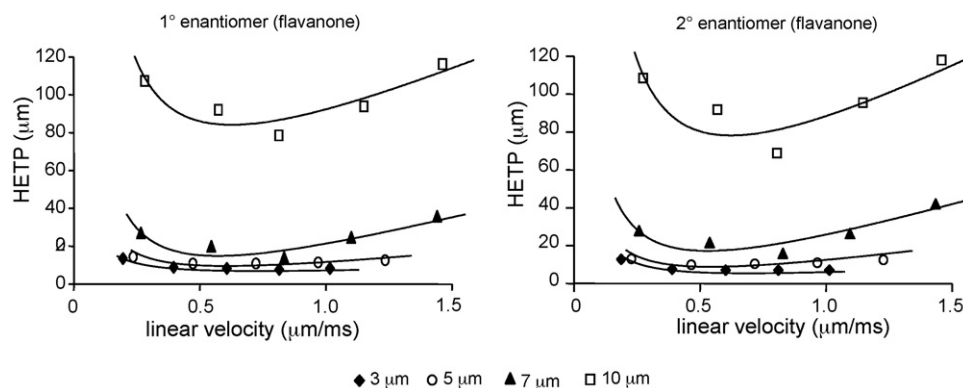


Fig. 5. Dependence of peak efficiency on the linear flow rate of the mobile phase in CEC for packing materials prepared based on the aminopropylsilanized silica with 3, 5, 7, 10 μm nominal particle size. Chiral selector coating and pore size were 25% (w/w) and 100 nm, respectively. Experimental conditions: mobile phase: 500 mM NH_4Ac , pH 5.5/MeOH/ACN, 1/49/50 (v/v/v); applied voltage -5 to -25 kV. Other conditions were as for the experiments shown in Fig. 3.

pared with the material of 5 μm nominal particle size. This is a clear indication of lower peak broadening due to decreased longitudinal inhomogeneity of the flow with smaller particles. Together with the A-term, the C-term was also somehow lower in the case of 3 μm material. This may be caused by shorter diffusion paths but may also be not directly related to the particle size of the materials, since peak retention was lower with 3 μm material. This means, a most likely somewhat lower actual loading of the chiral selector on 3 μm particles. Significantly higher values of van Deemter coefficients were observed in nano-LC experiments compared with CEC (Table 1). This indicates that the higher longitudinal homogeneity of the flow and significant intra-particle flow contribute to the higher peak efficiency observed in CEC separations.

3.4. The effect of pore size of silica on separation performance in CEC

With increasing pore size of silica the EOF increases as shown in Fig. 3. In addition, at least in CEC experiments, the contribution of the intra-particle flow in the overall flow increases and this should lead to increased peak efficiency. This has been shown in several studies previously [26,33,37]. The dependences of the peak efficiency on the linear flow rate of the mobile phase for the materials with various nominal pore sizes showed a clear increase of peak efficiency in the range from 30 to 200 nm (Fig. 6). The values of van Deemter coefficients shown in Table 2 indicate an unambiguous effect of the pore size on the C-term that is due to mass transfer

between the mobile and stationary phase. Increased intra-particle flow with increasing pore sizes of silica contributes to a faster mass transfer and by this way improves peak efficiency. This was true for both enantiomers of the analytes (Table 2).

A significant increase of the peak efficiency was observed with increasing pore sizes of the packing material also in nano-LC experiments (data not shown). This can be related to the accessibility of the interstitial surface by the analytes as well as to some intraparticle flow due to pressure gradients.

3.5. The effect of polysaccharide loading onto silica on separation performance in nano-LC and CEC

Coated-type polysaccharide-based CSPs offer the advantage of easy loading of silica with variable amounts of polysaccharide derivatives. This is useful in order to adjust the analyte retention and separation characteristics in chromatographic separations. In addition, the EOF depends significantly on the loading of neutral chiral selectors onto silica in CEC (see Fig. 3b).

In order to investigate the effect of chiral selector loading on the chromatographic performance, the studies were performed with capillaries packed with native silica particles coated with amylose tris(5-chloro-2-methylphenylcarbamate) at concentrations of 5, 10, 15 and 25% (w/w). The experiments were performed in both, the CEC and the nano-LC mode.

The effect of chiral selector loading on the analyte retention, separation factor of enantiomers, peak efficiency and resolution is

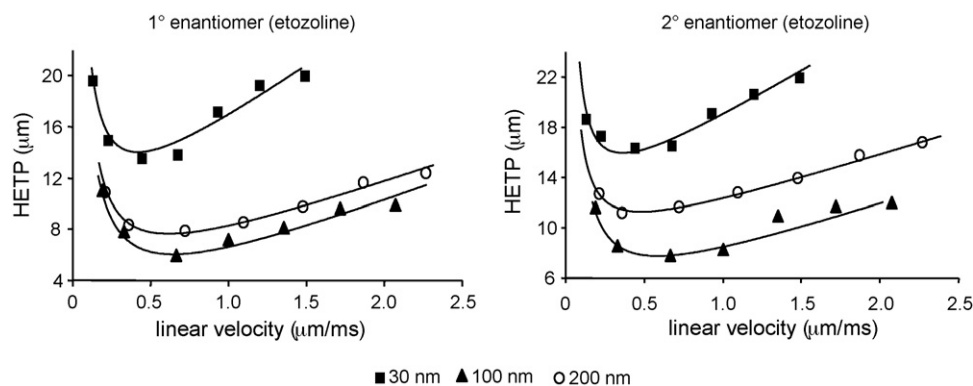


Fig. 6. Dependence of peak efficiency of etozoline enantiomers on the linear flow rate of the mobile phase in CEC for packing materials prepared based on the native silica materials with 30, 100 and 200 nm nominal pore size. Chiral selector coating was 25% (w/w). Applied voltage 3–30 kV. Other conditions were as for the experiments shown in Fig. 3a.

Table 2
The values of van Deemter coefficients for flavanone and etozoline enantiomers in CEC with packing materials of 30, 100 and 200 nm nominal pore size (Nominal particle size 5 μm).

Analyte	Nominal pore size, nm	First enantiomer			Second enantiomer		
		A, μm	B, $\mu\text{m}^2/\text{ms}$	C, ms	A, μm	B, $\mu\text{m}^2/\text{ms}$	C, ms
Etozoline	30	5.86	1.61	9.39	11.54	0.84	6.75
	100	1.26	1.71	4.01	2.95	1.46	4.35
	200	2.75	1.51	4.05	7.51	0.88	3.98
Flavanone	30	5.49	1.77	7.34	5.99	1.74	7.11
	100	3.78	1.53	2.73	4.92	1.34	3.26
	200	3.40	2.05	2.69	4.51	1.91	3.80

Silica was coated with 25% (w/w) chiral selector. For CEC conditions: see legend to Fig. 6.

Table 3
Separation characteristics of studied analytes with packing materials prepared based on native silica support with 5 μm nominal particle size, 100 nm nominal pore diameter and containing various amount of chiral selector.

Chiral selector (%)	Analyte	CEC, linear velocity, $\mu\text{m}/\text{ms}$	Nano-LC linear velocity, $\mu\text{m}/\text{ms}$	k_1		k_2		R_s		α		N_1/m		N_2/m	
				CEC	Nano-LC	CEC	Nano-LC	CEC	Nano-LC	CEC	Nano-LC	CEC	Nano-LC	CEC	Nano-LC
5	Etozoline	0.86	0.84	0.03	0.03	0.05	0.06	1.32	<0.5	1.90	1.79	215388	–	187740	–
	Flavanone			0.05	0.07	0.09	0.11	1.80	0.75	1.74	1.68	160344	–	154920	–
	Temazepam			0.05	0.06	0.33	0.37	6.92	2.65	6.72	5.90	173572	52028	30428	14251
10	Etozoline	0.86	0.84	0.04	0.05	0.07	0.08	1.47	<0.5	1.74	1.53	163056	–	145692	–
	Flavanone			0.07	0.07	0.12	0.11	1.89	0.54	1.64	1.51	130080	–	118668	–
	Temazepam			0.08	0.10	0.45	0.39	8.25	2.79	5.38	4.08	133796	38023	32100	14125
15	Etozoline	0.75	0.74	0.06	0.07	0.11	0.12	2.04	0.52	1.81	1.60	140272	–	107004	–
	Flavanone			0.11	0.12	0.19	0.19	2.86	1.01	1.68	1.62	113840	–	118648	–
	Temazepam			0.11	0.12	0.67	0.60	10.07	4.37	6.05	5.08	102772	39090	25276	11303
25	Etozoline	0.68	0.69	0.17	0.19	0.31	0.34	4.89	2.56	1.82	1.79	126420	30312	116112	24256
	Flavanone			0.41	0.45	0.71	0.76	8.41	5.56	1.73	1.69	126700	41534	115068	31043
	Temazepam			0.29	0.30	1.71	1.77	18.03	10.71	5.90	5.90	126092	36689	28272	13862

For experimental conditions, see Fig. 8.

summarized in Table 3. As expected the retention increased but the peak efficiency decreased with increasing loading of the chiral selector onto the surface of the silica particles [26,32,33].

The lower efficiency observed at higher chiral selector loading is most likely due to the hindered mass-transfer between the stationary and the mobile phase [26,32,33]. This can be clearly seen from Fig. 7 and Table 4. Thus, the C-term increased from 1.27 to 4.01 and 1.36 to 4.35 for the first and the second enantiomer of etozoline, respectively, with increasing the chiral selector loading from 5 to 25% (w/w) (Table 4). The same trend for the C-term was observed also for the enantiomers of flavanone (Fig. 7 and Table 4).

The effect of chiral selector concentrations on enantiomeric resolution in nano-LC was similar to that observed in CEC (results not shown).

3.6. Comparative enantioseparations in CEC and nano-LC

As mentioned in the Introduction, performing CEC experiments instead of nano-LC experiments is only reasonable if a real gain in peak efficiency can be observed. This was not always the case in papers published in the last few years on CEC. To answer the question about higher peak efficiency in CEC separations, the current experiments were performed by using the same capillary columns in both techniques, nano-LC and CEC. For this purpose the native silica-based CSP with 25% w/w chiral selector was used for the enantiomeric separation of all four racemic analytes under this study. At least 2-times higher peak efficiencies were observed in CEC separations compared to nano-LC separations (Fig. 8).

The effect of the linear flow rate on plate height in CEC and nano-LC is shown in Fig. 9a and b, respectively. The minimum

Table 4
The values of van Deemter coefficients for etozoline and flavanone enantiomers in CEC with packing materials prepared based on native silica support with 5 μm nominal particle size, 100 nm nominal pore diameter and containing various amount of chiral selector.

Analyte	Loading of chiral selector, % (w/w)	First enantiomer			Second enantiomer		
		A, μm	B, $\mu\text{m}^2/\text{ms}$	C, ms	A, μm	B, $\mu\text{m}^2/\text{ms}$	C, ms
Etozoline	5	1.16	2.04	1.27	2.10	1.80	1.36
	10	1.92	2.06	1.91	2.10	2.24	2.46
	25	1.26	1.71	4.01	2.96	1.46	4.35
Flavanone	5	2.39	2.52	1.03	2.19	2.58	1.40
	10	3.35	2.57	1.64	4.40	2.35	1.69
	25	3.78	1.53	2.73	4.93	1.34	3.26

For experimental conditions, see Fig. 7.

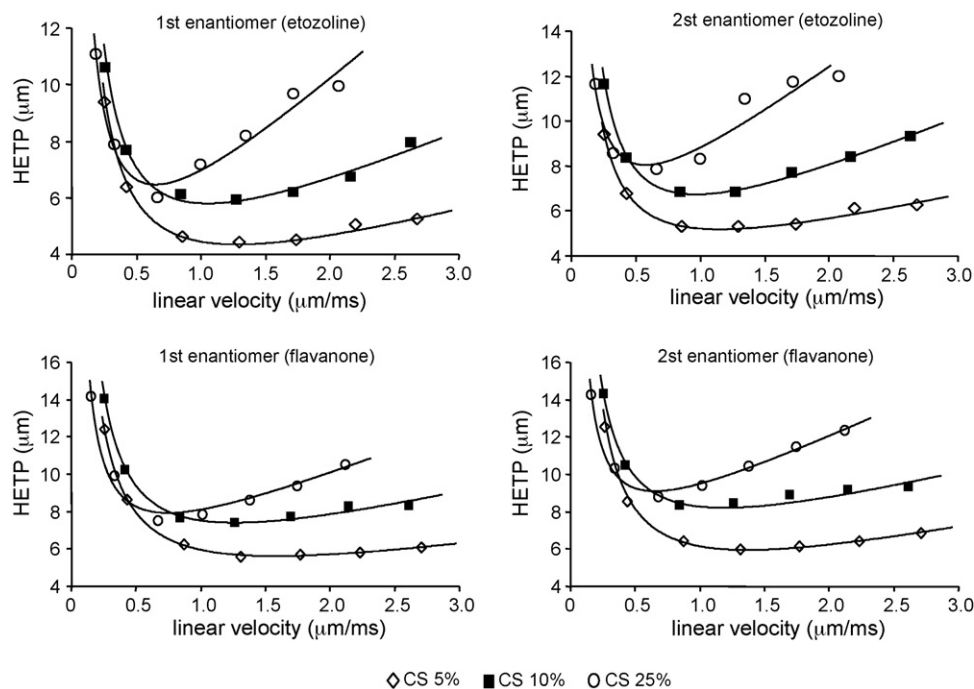


Fig. 7. Dependence of peak efficiency on the linear flow rate of the mobile phase in CEC for packing materials prepared based on the native silica materials of 5 μm nominal particle size and 100 nm nominal pore diameter with 5, 10 and 25% (w/w) loading of the chiral selector. Applied voltage 3–30 kV. Other conditions were as for the experiments shown in Fig. 3a.

plate heights (7.86 μm and 22.41 μm) for the first enantiomer of flavanone were observed at linear flow rates of 0.75 μm/ms and 0.32 μm/ms in CEC and nano-LC, respectively. Based on these data one can conclude that CEC is a more efficient technique for the separation of enantiomers compared to nano-LC. The shape of the van Deemter curve observed in CEC was also flatter especially in the range of higher linear flow rates. Indeed, in CEC the significant intra-particle flow of the analytes might be responsible for the improved mass-transfer. This means a lower C-term in the van Deemter equation [26,32,33]. Actually, the C-term was

50.35 and 63.35 for the first and the second peaks of etozoline in nano-LC, while the values were 4.02 and 4.21 in CEC. The same trends were observed also for the enantiomers of flavanone and temazepam. A- and B-terms were also favourable in CEC compared to nano-LC (data not shown) although the data were not as straightforward (especially for B-term) as in the case of the C-term. Thus, a plug-like profile of the electrokinetically driven flow and low contribution of longitudinal diffusion were most likely responsible for the lower peak-broadening in CEC versus nano-LC.

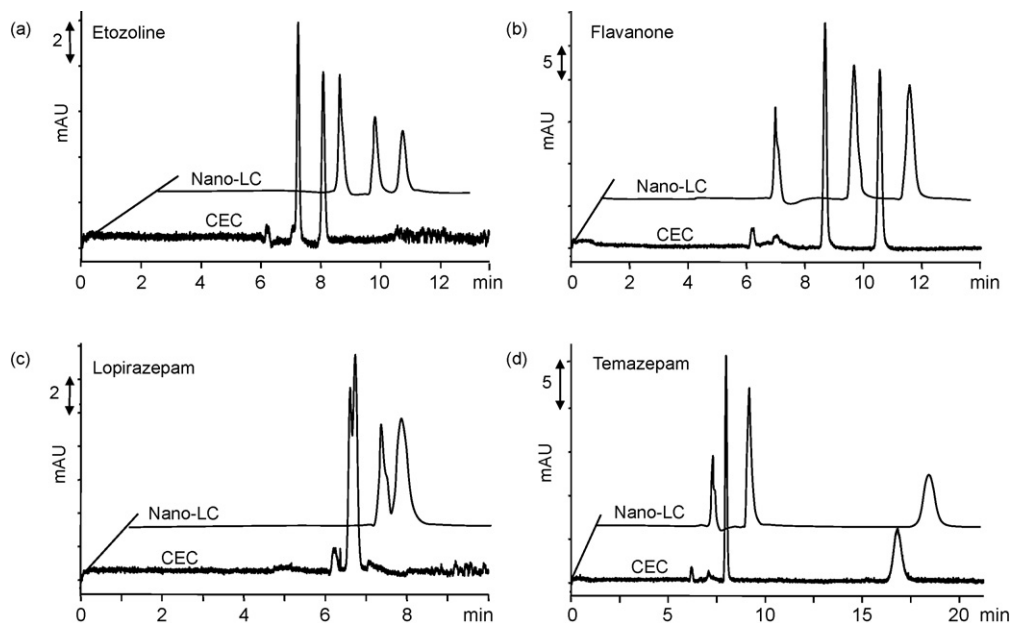


Fig. 8. Comparative enantioseparations of etozoline, flavanone, lopirazepam and temazepam in nano-LC and CEC. Experimental conditions: sample, etozoline and temazepam at 0.1 mg/mL, flavanone at 0.05 mg/mL, lopirazepam at 0.02 mg/mL. Mobile phase, 500 mM NH₄Ac, pH 5.5/water/methanol/acetonitrile, 1/4/25/70 (v/v/v/v); detection at 214 nm. Nano-LC flow rate and injected volume, 210 nL/min and 60 nL, respectively. CEC applied voltage, 10 kV; for other conditions, see Fig. 3a.

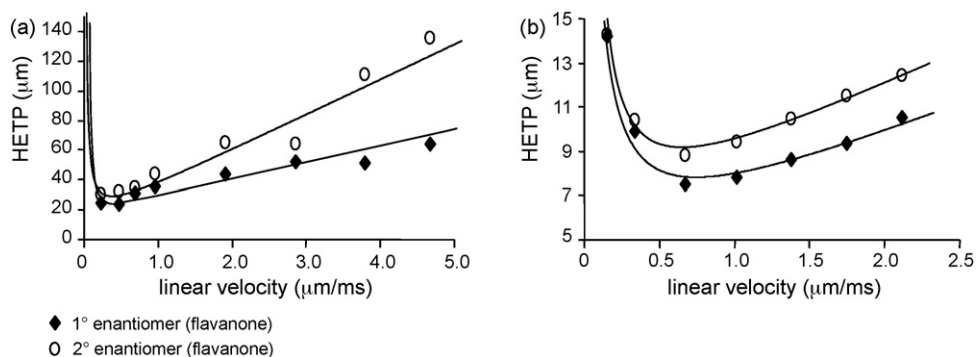


Fig. 9. Dependence of the plate height on the linear flow velocity of the mobile phase in nano-LC (a) and CEC (b) separation of flavanone enantiomers. Stationary phase: native silica (5 μm , 100 nm) coated with 25% (w/w) chiral selector. Nano-LC conditions: injection volume, about 60 nL; flow rate 100–1300 nL/min. CEC conditions, 3–30 kV. For other conditions, see Fig. 3a.

4. Conclusions

From the results of this study it can be concluded that capillary columns packed with silica coated with amylose tris(5-chloro-2-methylphenylcarbamate) can be used for miniaturized pressure- and electro-driven enantioseparations. The separation characteristics were affected by the particle and pore size of used silica materials, as well as by the amount of coated polysaccharide derivative. CEC appears to be an advantageous technique from the viewpoint of peak efficiency and resolution. Further comparative mechanistic studies between nano-LC and CEC separations are required for a better understanding of the origin of the higher separation efficiency in CEC separations and optimization of the preparation technology of chiral CEC columns.

Acknowledgements

B.C. thanks Georgia National Science Foundation (GNSF) for providing partial financial support for this study (Project No. GNSF/ST 06/-071). Sh.S. thanks the same GNSF for providing the Presidential Grant for Young Scientists (GNSF/PRES07/4-154).

References

- [1] D. Wistuba, V. Schurig, *Electrophoresis* 21 (2000) 4136.
- [2] S. Fanali, B. Chankvetadze, P. Catarcini, G. Blaschke, *Electrophoresis* 22 (2001) 3131.
- [3] B. Chankvetadze, *J. Sep. Sci.* 24 (2001) 691.
- [4] M. Lämmerhofer, F. Svec, J.M.J. Fréchet, W. Lindner, *TrAC-Trends Anal. Chem.* 19 (2001) 676.
- [5] P. Sajonz, X. Gong, W.R. Leonard Jr., M. Biba, C.J. Welch, *Chirality* 18 (2006) 803.
- [6] C.J. Welch, P. Sajonz, M. Biba, J. Gouker, J. Fairchild, *J. Liq. Chromatogr. Rel. Technol.* 29 (2006) 2185.
- [7] P. Sajonz, W. Schafer, S. Shultz, T. Rosner, C.J. Welch, *J. Chromatogr. A* 1145 (2007) 149.
- [8] C.J. Welch, *Chirality* 21 (2009) 114.
- [9] W.H. Pirkle, P.G. Murray, *J. Chromatogr.* 641 (1993) 11.
- [10] S. Allenmark, B. Bomgren, H. Boren, *J. Chromatogr.* 264 (1983) 63.
- [11] J. Hermansson, *J. Chromatogr.* 269 (1983) 71.
- [12] T. Ward, D.W. Armstrong, in: M. Zief, L.J. Crane (Eds.), *Chromatographic Chiral Separations*, Chromatographic Science Series, vol. 40, Marcel Dekker, New York, 1988 (Chapter 5, p. 131).
- [13] I. Kartoza, G. D'Orazio, B. Chankvetadze, S. Fanali, *J. Cap. Elec. Microchip Tech.* 9 (2005) 31.
- [14] Y. Okamoto, S. Honda, I. Okamoto, H. Yuki, *J. Am. Chem. Soc.* 103 (1981) 6971.
- [15] G. Blaschke, B. Brocker, W. Fraenkel, *Angew. Chem. Int. Ed. Engl.* 25 (1986) 830.
- [16] Y. Okamoto, M. Kawashima, K. Hatada, *J. Am. Chem. Soc.* 106 (1984) 5357.
- [17] B. Chankvetadze, E. Yashima, Y. Okamoto, *Chem. Lett.* (1993) 617.
- [18] Y. Okamoto, E. Yashima, *Angew. Chem.* 37 (1998) 1021.
- [19] B. Chankvetadze, E. Yashima, Y. Okamoto, *J. Chromatogr. A* 670 (1994) 39.
- [20] B. Chankvetadze, L. Chankvetadze, Sh. Sidamonidze, E. Yashima, Y. Okamoto, *J. Pharm. Biomed. Anal.* 13 (1995) 695.
- [21] B. Chankvetadze, L. Chankvetadze, Sh. Sidamonidze, E. Yashima, Y. Okamoto, *J. Pharm. Biomed. Anal.* 14 (1996) 1295.
- [22] E. Francotte, M. Jung, *Chromatographia* 42 (1996) 521.
- [23] K. Krause, M. Girod, B. Chankvetadze, G. Blaschke, *J. Chromatogr. A* 837 (1999) 51.
- [24] L. Chankvetadze, I. Kartoza, C. Yamamoto, B. Chankvetadze, G. Blaschke, Y. Okamoto, *Electrophoresis* 23 (2002) 486.
- [25] K. Otsuka, C. Mikami, S. Terabe, *J. Chromatogr. A* 887 (2000) 457.
- [26] B. Chankvetadze, I. Kartoza, J. Breittkreutz, Y. Okamoto, G. Blaschke, *Electrophoresis* 22 (2001) 3327.
- [27] M. Girod, B. Chankvetadze, Y. Okamoto, G. Blaschke, *J. Sep. Sci.* 24 (2001) 27.
- [28] B. Chankvetadze, I. Kartoza, C. Yamamoto, Y. Okamoto, G. Blaschke, *J. Pharm. Biomed. Anal.* 30 (2003) 1897.
- [29] L. Chankvetadze, I. Kartoza, C. Yamamoto, B. Chankvetadze, G. Blaschke, Y. Okamoto, *J. Sep. Sci.* 25 (2002) 653.
- [30] B. Chankvetadze, E. Yashima, Y. Okamoto, *J. Chromatogr. A* 694 (1994) 101.
- [31] B. Chankvetadze, L. Chankvetadze, Sh. Sidamonidze, E. Kasashima, E. Yashima, Y. Okamoto, *J. Chromatogr. A* 787 (1997) 67.
- [32] S. Fanali, G. D'Orazio, K. Lomsadze, B. Chankvetadze, *J. Chromatogr. B* 875 (2008) 296.
- [33] B. Chankvetadze, I. Kartoza, J. Breittkreutz, M. Knobloch, Y. Okamoto, G. Blaschke, *J. Sep. Sci.* 24 (2001) 251.
- [34] B. Chankvetadze, G. Blaschke, *Electrophoresis* 21 (2000) 4159.
- [35] K. Krause, B. Chankvetadze, Y. Okamoto, G. Blaschke, *J. Microcol. Sep.* 12 (2000) 398.
- [36] M. Girod, B. Chankvetadze, G. Blaschke, *Electrophoresis* 22 (2001) 1282.
- [37] B. Chankvetadze, I. Kartoza, Y. Okamoto, G. Blaschke, *J. Sep. Sci.* 24 (2001) 635.